

Dynamic Changes in Dimensional Structures of Co-Complex Crystals

Atsushi Kondo,^{†‡} Tomohiro Nakagawa,[‡] Hiroshi Kajiro,^{§*} Ayako Chinen,[‡] Yoshiyuki Hattori,[⊥] Fujio Okino,[⊥] Tomonori Ohba,[‡] Katsumi Kaneko,^{¶¶} and Hirofumi Kanoh^{‡*}

[†] Collaborative Innovation Center for Nanotech FIBER (nanoFIC), Shinshu University, Ueda Nagano 386-8567, Japan, [‡] Graduate School of Science, Chiba University, Yayoi, Inage, Chiba 263-8522, Japan, [§] Nippon Steel Corporation, Shintomi, Futtsu, Chiba 293-8511, Japan, and [⊥] Department of Chemistry, Faculty of Textile Science and Technology, Shinshu University, Ueda 386-8567, Japan.

* To whom correspondence should be addressed. E-mail: kanoh@pchem2.s.chiba-u.ac.jp, kajiro.hiroshi@nsc.co.jp

[†] Present address: Department of Applied Chemistry, Tokyo University of Agriculture and Technology, 2-24-16 Naka-cho, Koganei, Tokyo 184-8588, Japan.

^{¶¶} Present address: Institute of Carbon Science & Technology, Shinshu University, Wakasato 4-17-1, Nagano, 380-8553, Japan.

Supporting online materials

About crystal $\{[\text{Co}(\text{bpy})_2(\text{CH}_3\text{CN})_2(\text{H}_2\text{O})_2]\cdot 2(\text{OTf})\}$ (1**) (bpy = 4,4'-bipyridine, OTf = trifluoromethanesulfonate):**

The crystal **1** has water and acetonitrile molecules in the crystal and they can be removed by the heating treatment. The temperature programmed desorption mass (TPD-mass) measurement was conducted in the temperature range from 323 K to 473 K with the heating rate of 3 K/min under He flow to search the removal process of the molecules (Figure 1S). The large peaks assigned at H_2O ($M = 18$) and CH_3CN ($M = 41$) were detected and they were removed at around 373 K (100 °C). However, another peak for the removal of water molecules can be seen at about 343 K (70 °C). This may be by pre-desorption of water from other parts in the crystallites.

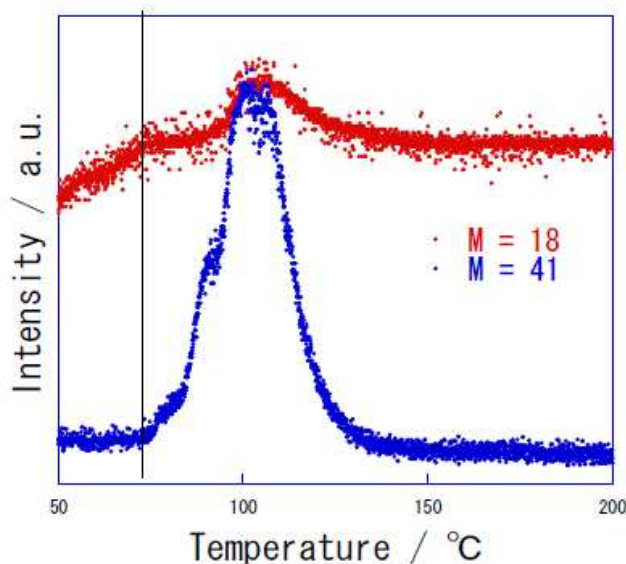


Figure 1S. TPD-mass spectra of **1** from 323 K (50 °C) to 473 K (200 °C).

Thermal gravimetric measurements were performed on a Seiko Instruments Inc. TG-DTA6200 under nitrogen gas flow (150 mL/min) (Figure 2S). Samples were heated from room temperature to 873 K, at a heating rate of 3 K/min. Thermal gravimetric analysis of **1** showed that coordinated acetonitrile and water molecules are removed at around 373 K (exp.; 15.1w%, calcd.; 15.0w%). A plateau region from 378 K to 473 K was observed, showing no weight loss and good thermal stability above 378 K up to 473 K. In further heating process, there are the three step drops corresponding to the removal of one bpy (exp; 20.3w%, calcd; 19.8w%), one bpy (exp; 20.6w%, calcd; 19.8w%), and two OTf without two fluorine atoms (exp.; 32.4w%, calcd.; 33.0w%). At last, CoF_2 was remained (exp.; 11.6w%, calcd.; 12.3w%). The stability of **1** was also checked by XRPD analysis. Although **1** was not stable in atmospheric condition, it was stable in the mother liquid over one year.

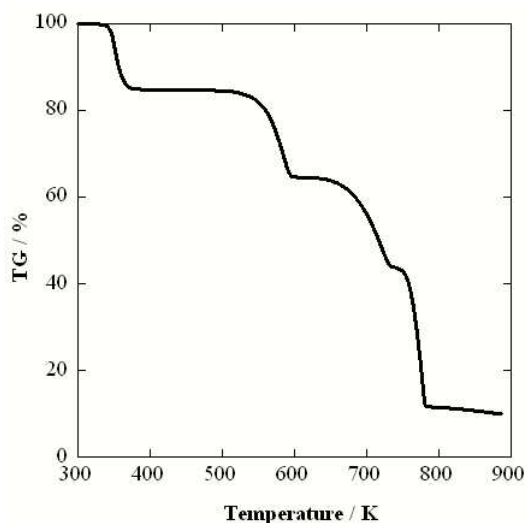


Figure 2S. TG curve of **1** from room temperature to 873 K.

Figure 3S shows the time course of XRPD pattern of **1** in vacuum. Although **1** can transform to **2**, $\{[\text{Co}(\text{bpy})(\text{OTf})_2(\text{H}_2\text{O})_2] \cdot (\text{bpy})\}$, in atmospheric conditions, **1** gradually loses the crystallinity in vacuum at room temperature, becoming an amorphous compound.

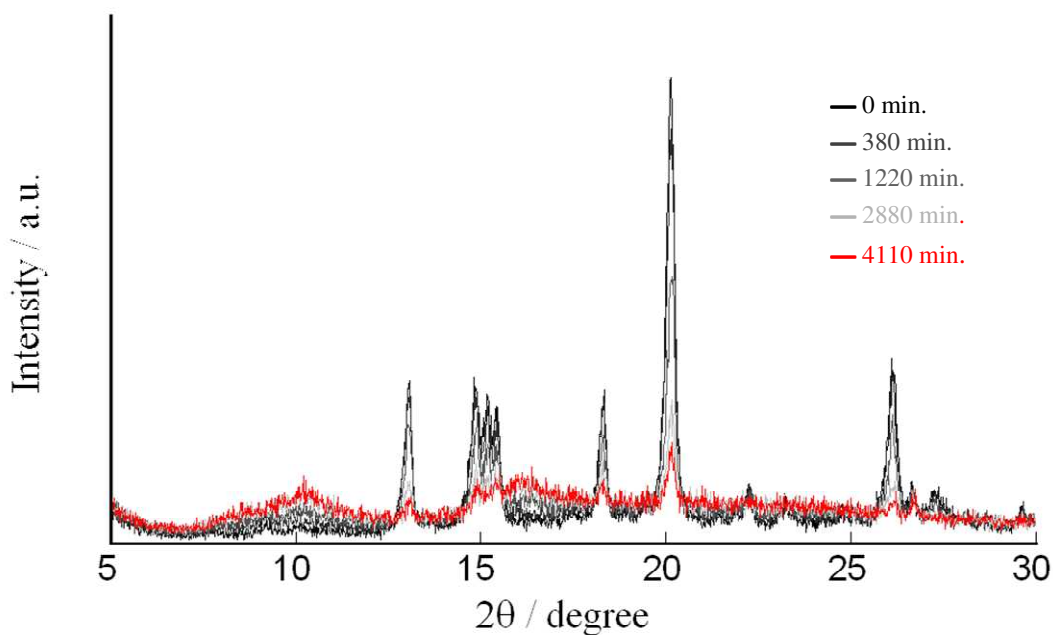


Figure 3S. Time course of XRPD pattern changes of **1** in vacuum ($\lambda = 1.5406 \text{ \AA}$).

About crystal **2**:

The crystal structural analysis of **2** was performed on the software EXPO 2004^[1S] with using a synchrotron XRD pattern ($\lambda = 1.002 \text{ \AA}$). The searched peaks were fed to the *n*-TREOR program^[2S] giving a reasonable solution of **2** with orthorhombic system, $a = 7.859$, $b = 15.056$, $c = 22.975 \text{ \AA}$, $M(20) = 30$, and $M(25) = 25$. The structural solution was performed on the XRD pattern of **3** to 70° (2θ) range with the

direct method. The cell parameters, background parameters, peak shift parameters, profile parameters, and structural parameters were refined using the Rietveld technique. All hydrogen atoms are located on the ideal positions. The final Rietveld refinement plot was shown in Figure 4S.

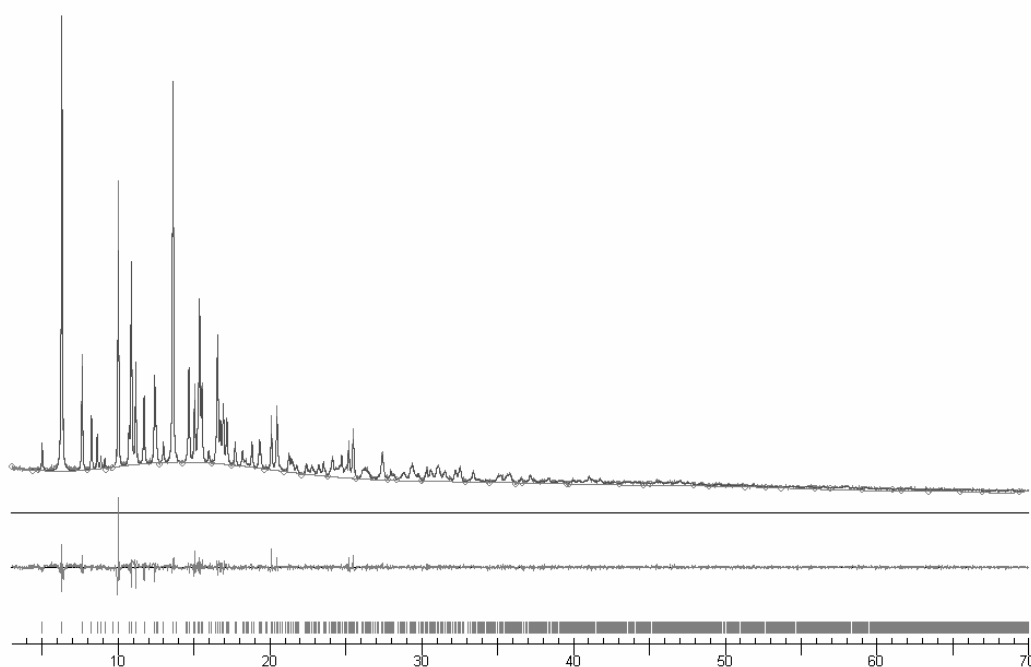


Figure 4S. Observed and calculated XRPD patterns of **2** in the 3-70° (2θ) range ($\lambda = 1.002 \text{ \AA}$). Difference plots and the reflection markers are shown at the bottom.

By the XRD analysis, **1** lost the coordinated acetonitrile molecules and transformed to the 1D chain compound (**2**). To confirm the removal of acetonitrile molecules in the presence of water molecules, TPD-mass measurement was performed (Figure 5S). Although the peak of water molecule is detected at between 423 K (150 °C) to 473 K (200 °C), the peak of acetonitrile molecule was not observed, supporting the removal of acetonitrile from **1**.

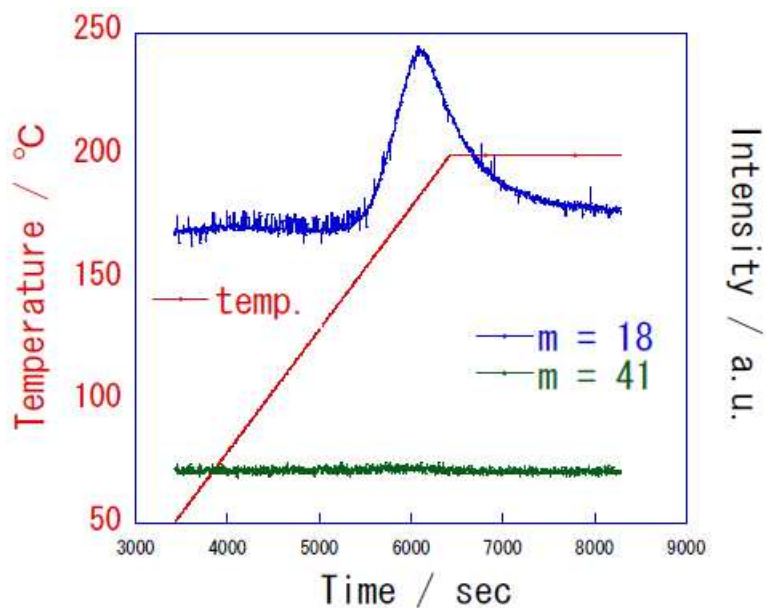


Figure 5S. TPD-mass spectra of **2** from room temperature to 473 K.

The TG analysis of **2** was performed at the range from room temperature to 900 K with the heating rate of 3 K/min under N₂ flow (150 mL/min) (Figure 6S). There are four weight drops corresponding to the removal of water (exp.; 5.6w%, calcd.; 5.12w%), one bpy (exp.; 22.0w%, calcd.; 22.1w%), one bpy (exp.; 23.1w%, calcd.; 22.1w%), and two OTf without two fluorine atoms (exp.; 35.1w%, calcd.; 37.8w%).

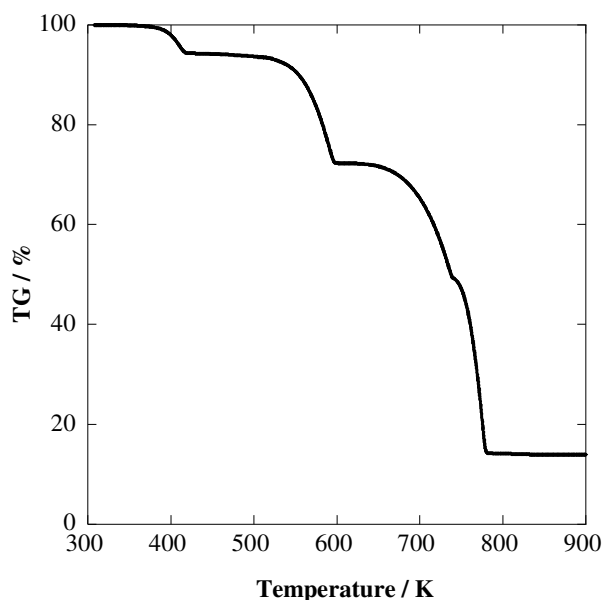


Figure 6S. TG curve of **2** from room temperature to 900 K.

About crystal [Co(bpy)₂(OTf)₂] (**3**):

The experimental XRPD patterns of **3** from **1** and from **2** are shown with the simulated X-ray diffraction (XRD) patterns of the as-synthesized and guest-free 2D sheet stacked types of compounds^[3S] solved by the single crystal XRD analysis in Figure 7S. The pattern of **3** is quite similar to both the simulated XRD

patterns, especially to the guest-free structure, showing similar framework structures each other, although the lower similarity at the higher diffraction angle region. This can be due to different measurement temperatures (**3**: room temp., single crystal: 173 K).

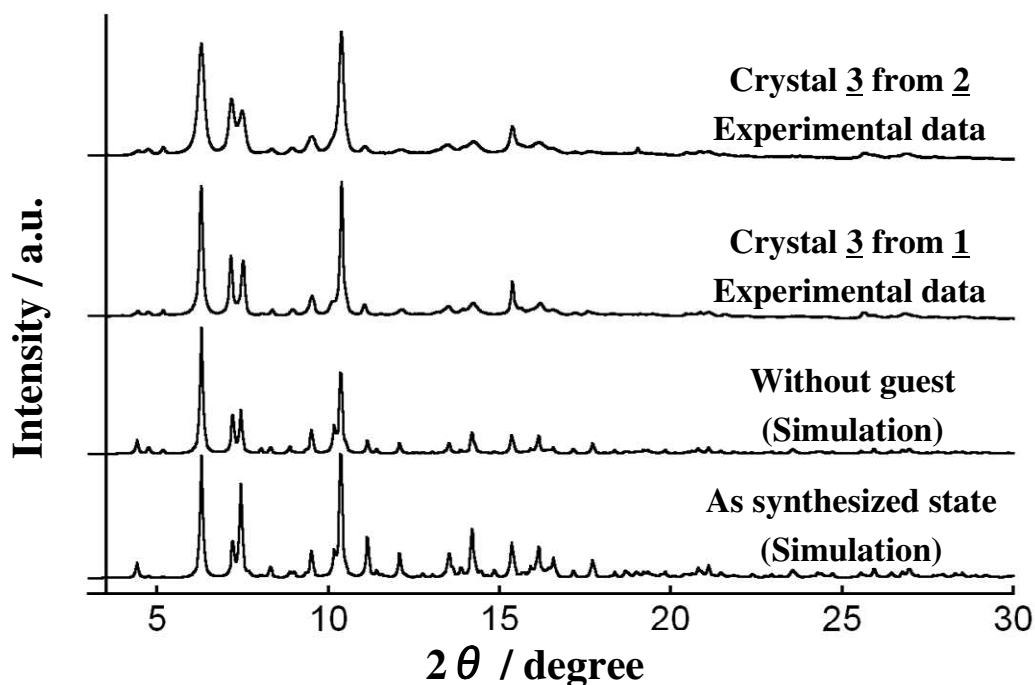


Figure 7S. Synchrotron XRD patterns of simulated and experimental **3** ($\lambda = 1.002 \text{ \AA}$).

Although the structure of **3** is almost the same to that of one that we previously reported, there is slight discrepancy between the XRD patterns of them. Then we performed the detail structural analysis of **3**. The unit cell parameters were searched by using DICVOL91 software^[35]. The crystal structural data of the similar crystal^[45] was used as an initial input. The Rietveld refinement was performed on the XRD pattern with 2 to 70 (2θ) range with RIETAN-2000 software^[55]. The final Rietveld refinement plot was shown in figure 8S.

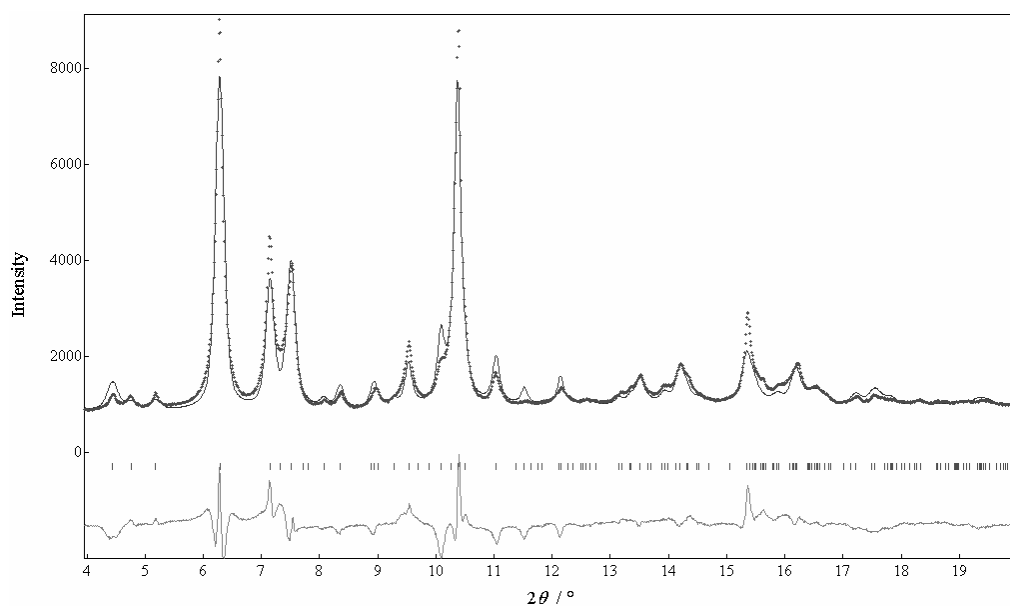


Figure 8S. Plot of the observed and calculated XRPD pattern of **3** in the 4-20° (2θ) range ($\lambda = 1.002 \text{ \AA}$). Difference plots and the reflection markers are shown at the bottom.

Crystal **3** was obtained from **1** or **2** by vacuum heating treatment. To check the presence/absence of water molecules, in situ infrared spectra of **1** and **3** were measured (Figure 9S). The crystal **3** was obtained by the heating at 423 K under vacuum for 2h. In the IR spectrum of **1**, the broad peak assigned to the O-H stretching vibration was confirmed at around 3500 cm^{-1} . On the other hand, the IR spectrum of **3** had no peak that can be assigned to the O-H stretching mode, showing the removal of water molecules by the vacuum heating treatment.

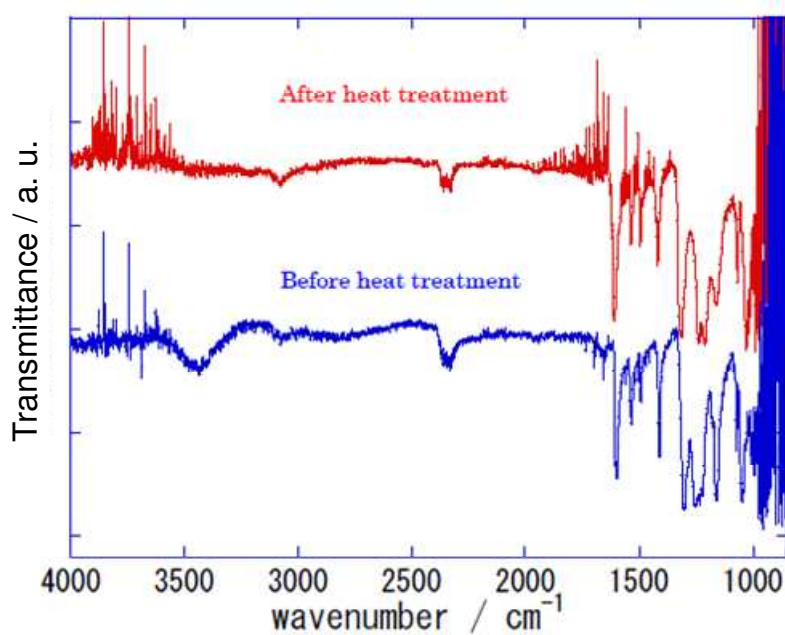


Figure 9S. IR spectrum of **1** (blue) and **3** (red).

Synchrotron X-ray diffraction patterns of 1, 2, and 3.

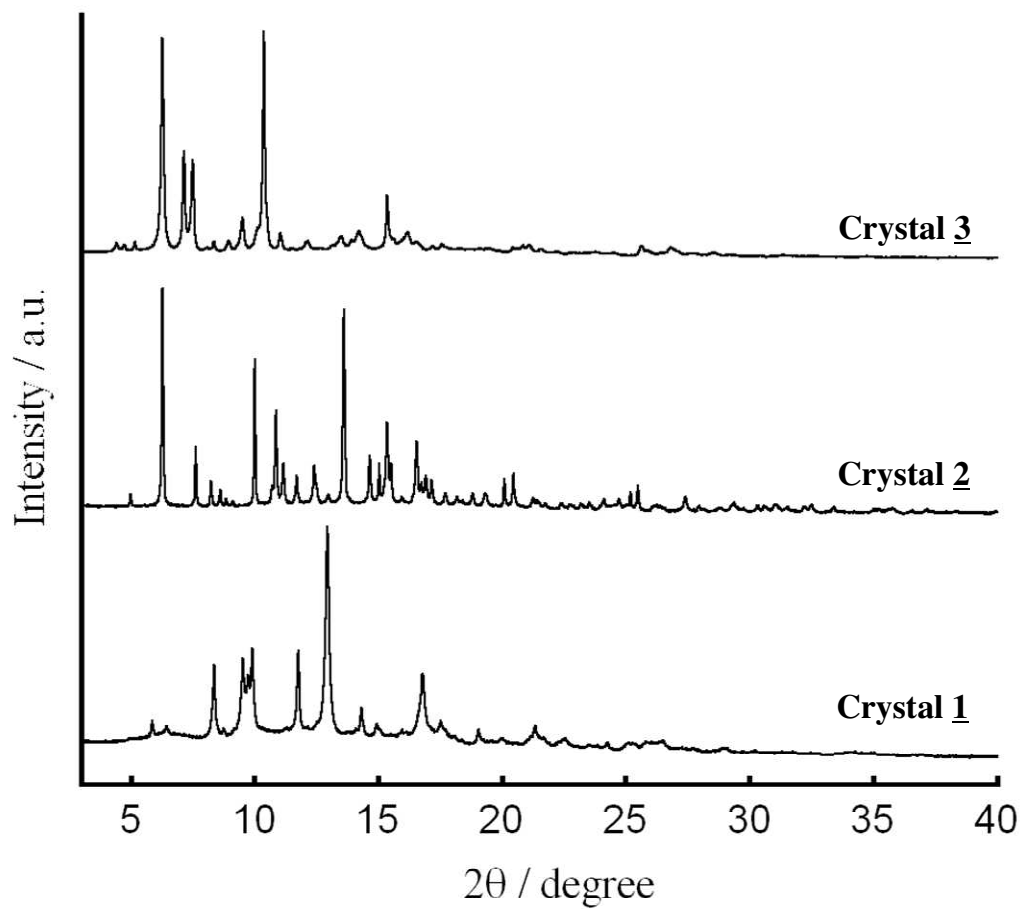
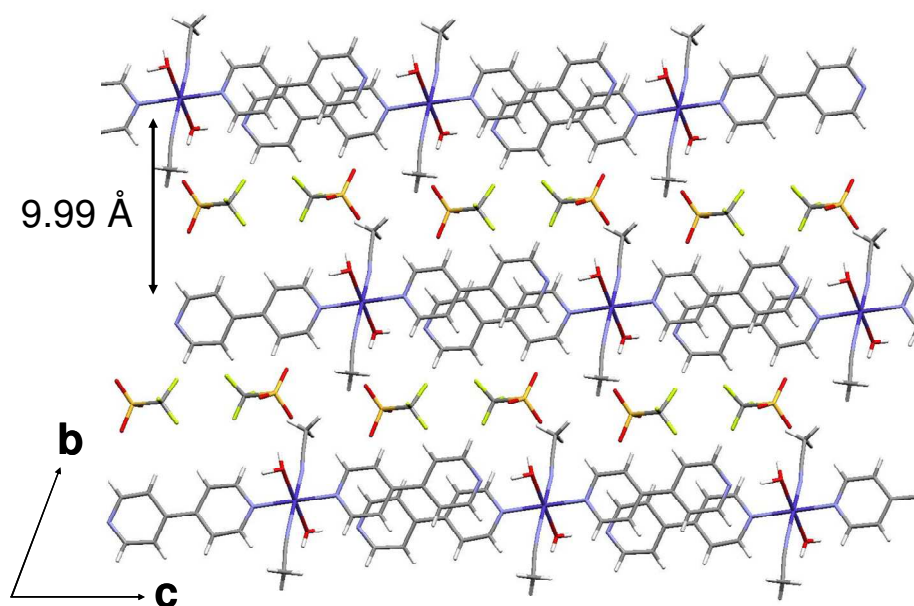


Figure 10S. Synchrotron XRPD patterns of 1, 2, and 3 ($\lambda = 1.002 \text{ \AA}$).

Crystal structure of 1, 2, and 3.



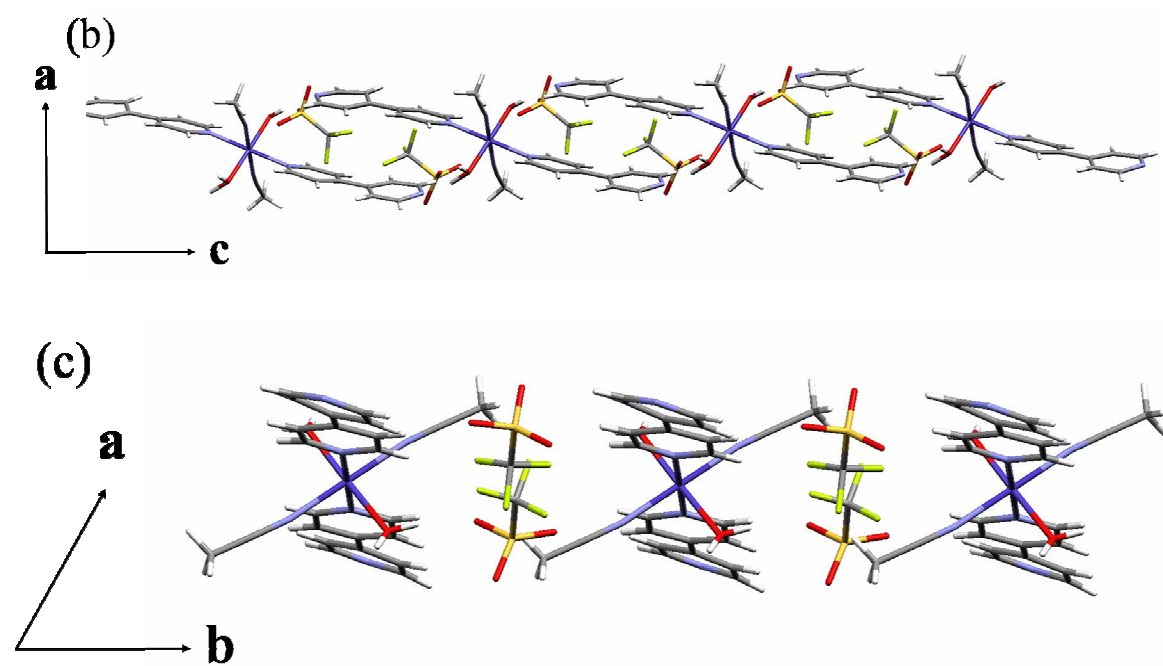
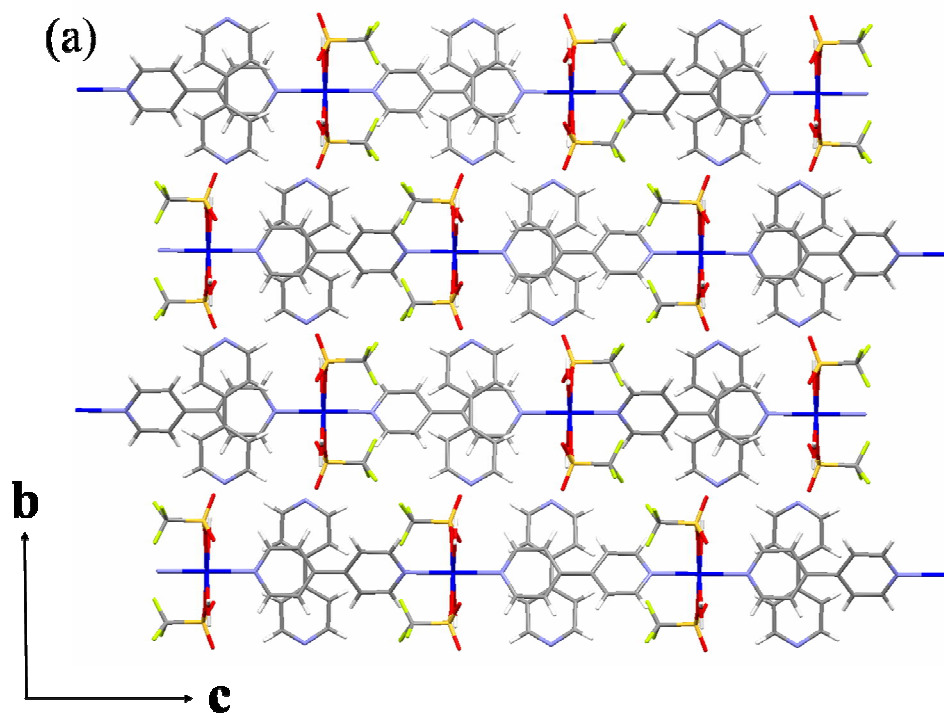


Figure 11S. (a) Crystal structure of **1** along *a* axis, (b) *b* axis, and (c) *c* axis.



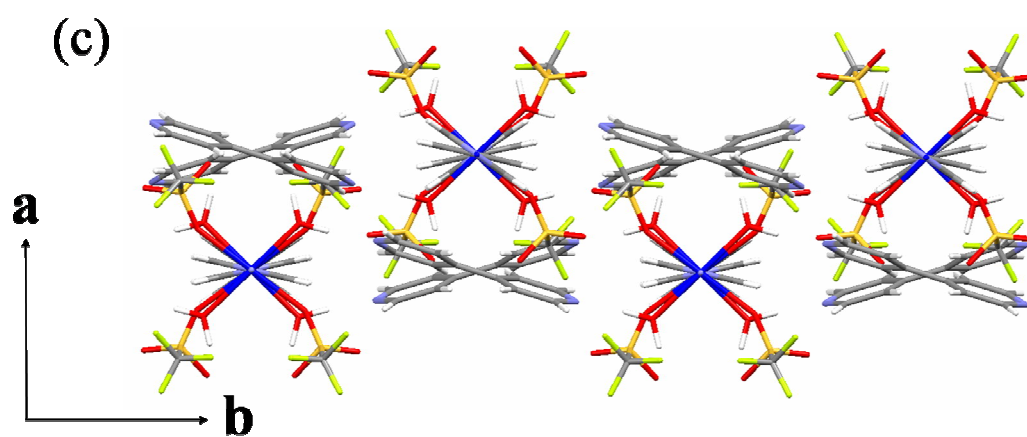
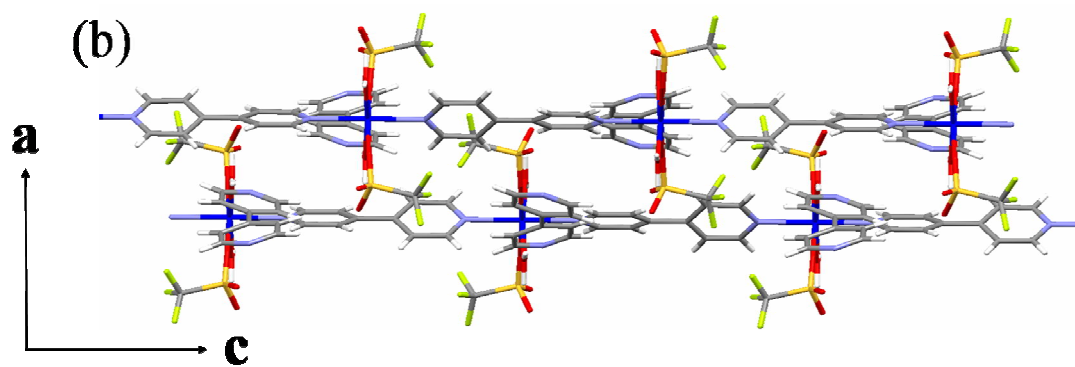
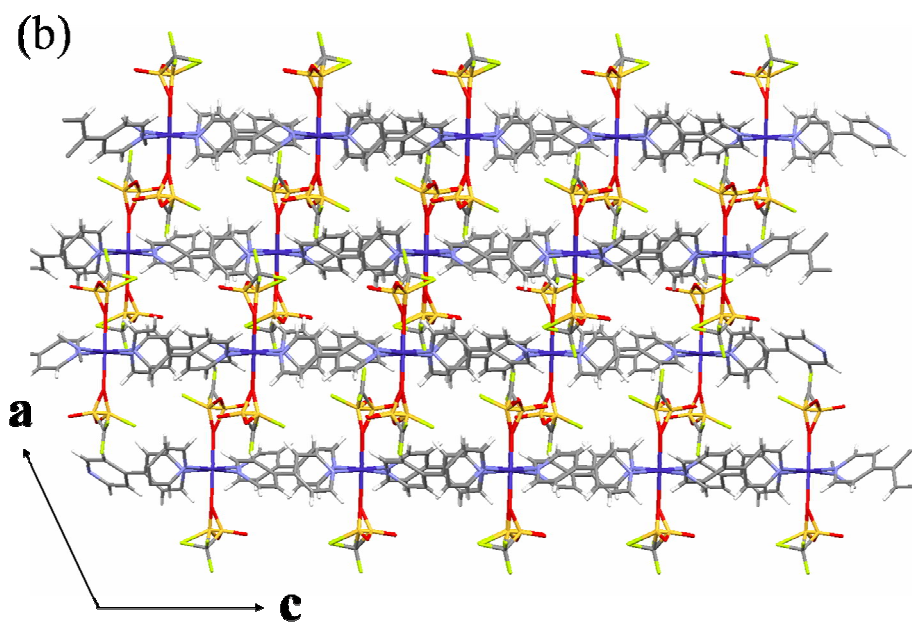
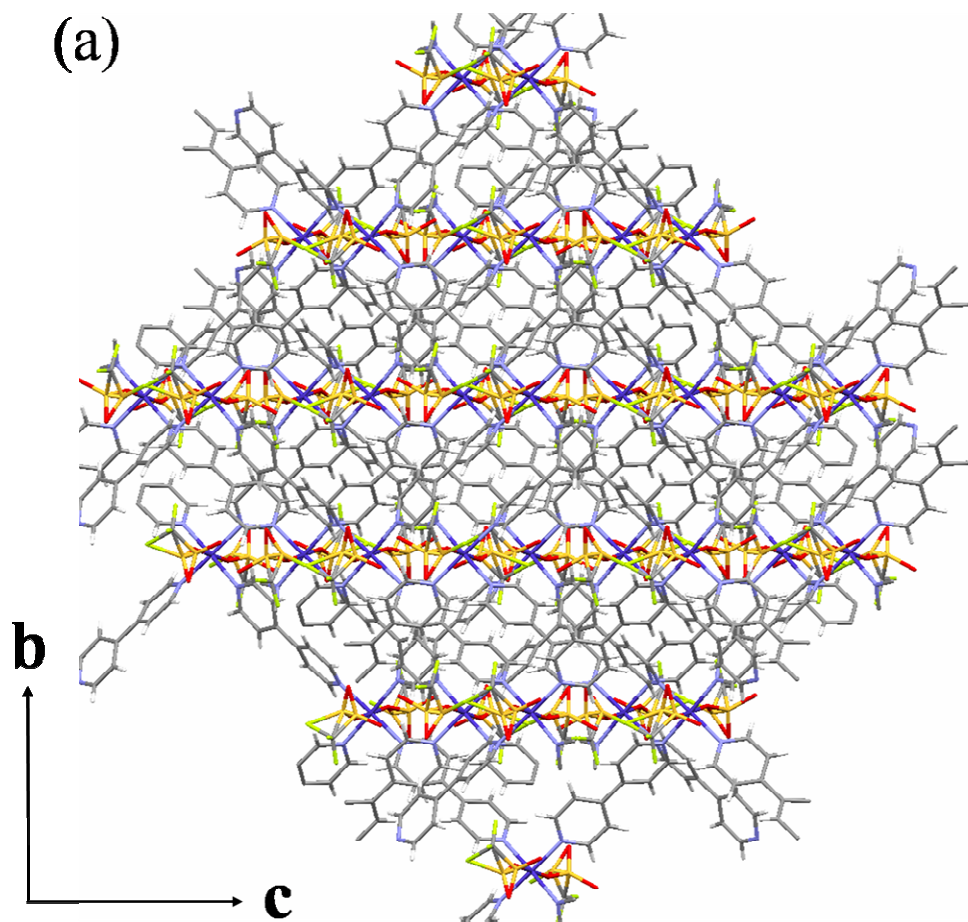


Figure 12S. (a) Crystal structure of **2** along *a* axis, (b) *b* axis, and (c) *c* axis.



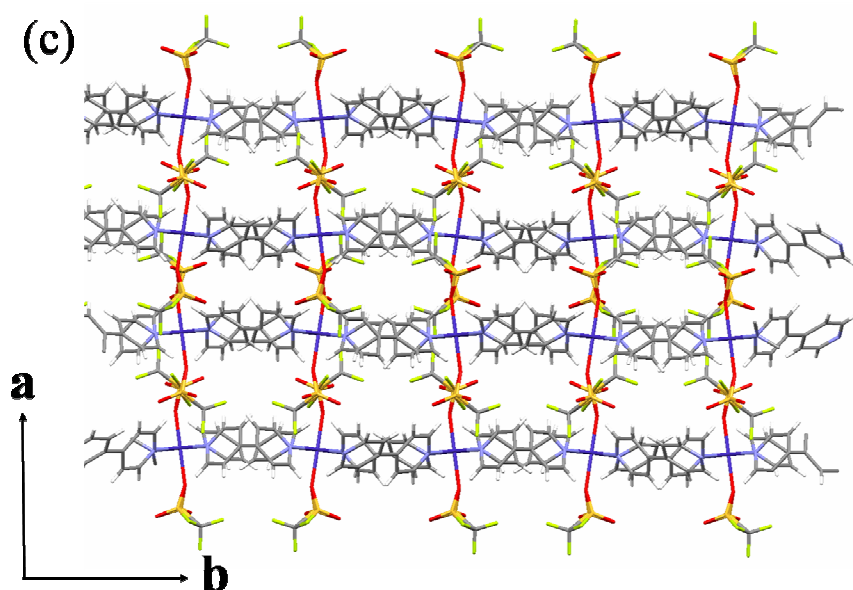


Figure 13S. (a) Crystal structure of **3** along *a* axis, (b) *b* axis, and (c) *c* axis.

Table 1S. Crystallographic data of **1**, **2**, and **3**.

Compound	1	2	3
Formula	C ₂₆ H ₂₆ CoF ₆ N ₆ O ₈ S ₂	C ₂₂ H ₂₀ CoF ₆ N ₄ O ₈ S ₂	C ₂₂ H ₁₆ CoF ₆ N ₄ O ₆ S ₂
<i>f</i> _w	787.58	705.49	669.46
Crystal system	Triclinic	Orthorhombic	Monoclinic
<i>a</i> , Å	7.0365(10)	7.854(5)	25.8872(17)
<i>b</i> , Å	10.5029(15)	15.051(5)	15.309(5)
<i>c</i> , Å	12.1466(17)	22.974(5)	16.8265(11)
<i>α</i> , deg	72.090(2)	90.000	90.000
<i>β</i> , deg	86.029(2)	90.000	111.219(1)
<i>γ</i> , deg	77.182(2)	90.000	90.000
<i>V</i> , Å ³	832.9(2)	2715.77	6216.37
Space group	<i>P</i> 1 (no. 1)	<i>Pccn</i> (no. 56)	<i>C</i> 2/ <i>c</i> (no. 15)
<i>Z</i>	1	4	8
<i>ρ</i> (calc), g cm ⁻³	1.570	1.726	1.431
Temp., K	298	Room temperature	Room temperature
<i>R</i> 1 (<i>I</i> > 2 <i>ρ</i> (<i>I</i>)) or <i>R</i> _p	0.0380	0.0242	0.0409
<i>wR</i> 2 (<i>I</i> > 2 <i>ρ</i> (<i>I</i>)) or <i>R</i> _w	0.0943	0.0351	0.0637
Completeness of data collection (< 50 deg)	93.2%	-	-

Analysis of N₂ adsorption isotherm.

The surface area was estimated by the N₂ adsorption at the pressure of $P/P_0 < 0.05$. By using DR (Dubinin- Radushkevich) analysis, the isosteric heat of adsorption, $q_{st, \phi=1/e}$, at the fractional filling ϕ of $1/e$ is led by adding the enthalpy of evaporation at the boiling point, ΔH_v on βE_0 . Here β is affinity coefficient and E_0 the characteristic adsorption energy. The pore parameters are listed in Table 2S.

Table 2S. Microporous parameters of **3** and ELM-22 (Co) ^[4S]

Species	Crystal 3	ELM-22 (Co)
Surface area [m ² g ⁻¹]	370	400
Micropore volume [mL g ⁻¹]	0.15	0.15
Total pore volume [mL g ⁻¹]	0.29	0.28
Isosteric heat of adsorption [kJ mol ⁻¹]	12.5	13.0

Surface areas are estimated with the adsorption branches of $P/P_0 < 0.05$, respectively.

References

- [1S] Altomare, A.; Burla, M. C.; Camalli, M.; Carrozzini, B.; Cascarano, G. L.; Giacobazzo, C.; Guagliardi, A.; Moliterni, A. G. G.; Polidori, G.; Rizzi, R. *J. Appl. Crystallogr.* **1999**, *32*, 339–340.
- [2S] Altomare, A.; Giacobazzo, C.; Guagliardi, A.; Moliterni, A. G. G.; Rizzi, R.; Werner, P.-E. *J. Appl. Crystallogr.* **2000**, *33*, 1180–1186.
- [3S] Boultif, A.; Louër, D. *J. Appl. Cryst.* **1991**, *24*, 987-993.
- [4S] Kondo, A.; Chinen, A.; Kajiro, H.; Nakagawa, T.; Kato, K.; Takata, M.; Hattori, Y.; Okino, F.; Ohba, T.; Kaneko, K.; Kanoh, H. *Chem. Eur. J.* **2009**, *31*, 7549-7553.
- [5S] Izumi, F.; Ikeda, T. *Mater. Sci. Forum*, **2000**, *198*, 321-324.